

Observational Constraints on Microwave Anisotropy from Point Sources

Eric Gawiser¹, Andrew Jaffe, & Joseph Silk

Departments of Physics and Astronomy and Center for Particle Astrophysics, University of California, Berkeley, CA 94720

ABSTRACT

Applying basic physical principles to recent observational results, we derive upper and lower limits on microwave anisotropy from point sources over the range of frequencies 10-1000 GHz. We examine the level of noise in the observations as a possible indication of source confusion at subarcminute scales. We also derive an upper limit on microwave anisotropy caused by the sources responsible for the Far-Infrared Background radiation detected in FIRAS data. Our upper limit on point source confusion of $\Delta T/T = 10^{-5}$ for a $10'$ beam at 100 GHz would cause severe foreground contamination for CMB anisotropy observations, although the actual contamination level is probably much lower. This upper limit constrains the long-feared possibility of an undetected population of sources with emission peaking near 100 GHz. Source detections closer to 100 GHz are needed to improve our knowledge of galaxy evolution at high redshift and to predict the level of point source confusion.

Subject headings: cosmic microwave background anisotropy – infrared: galaxies – far-infrared background

1. Introduction

The detection of anisotropy in the Cosmic Microwave Background by COBE DMR (Smoot et al. 1992) and several other instruments has generated interest in measuring CMB anisotropy on all angular scales with the goal of determining cosmological parameters. Improved instrumentation and the upcoming MAP (Microwave Anisotropy Probe) and Planck Surveyor² satellite missions focus current attention on angular scales between one-half and one-tenth of a degree, and there is theoretical motivation for undertaking future observations at even smaller scales (Hu & White 1997, Metcalf & Silk 1998, Jaffe & Kamionkowski 1998).

Because the antenna temperature contribution of a point source is inversely proportional to the solid angle of the beam, observations at higher angular resolution are

¹gawiser@astron.berkeley.edu

²<http://map.gsfc.nasa.gov> and <http://astro.estec.esa.nl/Planck/>

more sensitive to extragalactic foregrounds, including radio sources, low- and high-redshift infrared-bright galaxies, and the Sunyaev-Zel'dovich effect from galaxy clusters. The dominant contribution of the Galaxy to microwave anisotropy is from diffuse emission (Toffolatti et al. 1998, Finkbeiner et al. 1998). Until recent SCUBA observations, almost all sources observed from 10-1000 GHz were selected at higher or lower frequencies, so there was little direct knowledge of point source populations with emission peaking in this wide frequency range. Blain, Ivison, and Smail (1998, see also Blain, Ivison, Smail, & Kneib 1998 and Scott & White 1998) use models for high-redshift galaxies normalized to SCUBA counts at 353 GHz to predict anisotropy from extragalactic point sources down to 100 GHz, but this extrapolation is model-dependent. Previous predictions of the total point source contribution (Toffolatti et al. 1998, Toffolatti et al. 1995, Franceschini et al. 1989, Wang 1991) used galactic evolution models with specific assumptions about dust temperatures and luminosity evolution to predict the level of extragalactic foreground. More phenomenological approaches (Gawiser & Smoot 1997, hereafter GS97, Sokasian et al. 1998, hereafter SGMS, and Tegmark & Efstathiou 1996) lack information on infrared galaxies at high redshift and on dim but numerous radio sources.

Cosmic microwave background observations contain contributions to anisotropy from two groups of point sources. The bright sources at a level of at least 5σ (σ is the quadrature sum of instrument noise, CMB fluctuations, diffuse Galactic emission, and underlying point source fluctuations) can be detected individually and eliminated by masking the pixels containing them. This detection limit can be lowered by using prior knowledge of the locations of bright sources obtained from extrapolating far-infrared and radio frequency observations as described in GS97 and SGMS (as well as filtering, fourier transform, and wavelet techniques; see Tegmark & de Oliveira-Costa 1998, Ferreira & Maguiejo 1997, Tenorio et al. 1998). Numerous dimmer sources will add to anisotropy but cannot be detected without performing further observations at higher resolution at nearby frequencies. For most planned CMB observations, these simultaneous observations will be difficult due to large sky coverage at high resolution of the primary instrument (although Planck's wide frequency coverage will help with foreground subtraction.)

We utilize recent sub-arcminute resolution observations to constrain the contribution to anisotropy from this second group of point sources that will inevitably contaminate measurements of CMB anisotropy. Recent observations using BIMA by Wilner & Wright (1997) detected no sources brighter than 3.5 mJy in the 15 arcmin² of the Hubble Deep Field (HDF) at 4.7'' resolution at 107 GHz. We combine this constraint with the counts of sources detected in blank fields at 353 GHz by SCUBA (Hughes et al. 1998, Barger et al. 1998, Eales et al. 1998) and at 8.4 GHz with the VLA (Richards et al. 1998, Fomalont et al. 1997), with blank field upper limits from BIMA/OVRO at 28.5 GHz (Holzapfel 1998, Carlstrom 1998), SuZIE at 142 GHz (Church et al. 1998), IRAM at 250 GHz (Kreysa 1998, Grewing 1997), SCUBA at 667 GHz (Hughes et al. 1998), and CSO at 850 GHz (Phillips 1998), and with the detection of Far-Infrared Background radiation in FIRAS data (Puget et al. 1996, Burigana & Popa 1997, Fixsen et al. 1998).

It has long been feared that a population of sources with spectra peaking near 100 GHz, due to self-absorbed radio emission or thermal emission at very high redshift, might remain undetected by radio and far-infrared observations while contributing significantly to measurements of CMB anisotropy. Now that high-resolution observations are available in the frequency range relevant to CMB anisotropy observation, we set upper and lower limits on point source confusion between 10 and 1000 GHz by assuming that the emission of point sources originates from synchrotron, free-free, thermal dust, and spinning dust grain emission.

2. Extragalactic Point Sources

The main emission mechanism of bright far-infrared sources is graybody reradiation of starlight and/or Active Galactic Nuclei (AGN) radiation absorbed by dust. GS97 predict the level of microwave anisotropy from the 5319 low-redshift infrared-bright galaxies in the IRAS 1.2 Jy survey (Fisher et al. 1995). We expect there to be numerous higher-redshift starburst galaxies like the prototypes Arp 220, F 10214+4724, SMM 02399-1236 (Ivison et al. 1998), and APM 08279+5255 (Lewis et al. 1998) which generate similar dust emission, and with their spectra redshifted considerably these sources could easily be missed by far-infrared surveys and yet make significant contributions to the microwave sky. There may exist a population of ultraluminous proto-elliptical galaxies which cannot be described by models using smooth evolution of the IRAS luminosity function. Recent detections of the Far-Infrared Background radiation and of submillimeter sources by SCUBA (Smail, Ivison, & Blain 1998; Smail, Ivison, Blain, & Kneib 1998) give us the first clues about the nature and abundance of these high-redshift objects.

A separate population of extragalactic point sources are radio-loud, typically elliptical galaxies or AGN. Radio sources which have nearly flat spectra up through microwave frequencies are called blazars, a class which includes radio-loud quasars and BL Lacertae objects where synchrotron self-absorption due to the opacity of the dense nuclear regions at low frequencies prevents the spectrum from falling with frequency. SGMS examine 2200 bright radio sources in detail, but there are over ten thousand of these sources which are bright enough to have an impact on arcminute-resolution microwave observations.

For instruments of resolution $\geq 10'$, galaxy clusters will be unresolved and will provide an additional family of point sources via the Sunyaev-Zel'dovich effect (Sunyaev & Zel'dovich 1972). The observations used here are basically insensitive to SZ clusters as the fields have been chosen to avoid known clusters and are typically observed at sub-arcminute resolution. Anisotropy from SZ sources is not expected to seriously impair CMB anisotropy observations (Refregier, Spergel, & Herbig 1998, Aghanim et al. 1997).

3. Analysis

We assume for these calculations that observations use pixels of width equal to the FWHM of their beam. Overpixelization will lead to a small correction in the level of anisotropy and makes it easier to distinguish point sources, which contribute to several pixels, from instrument noise, which is often uncorrelated between neighboring pixels.

We can rigorously predict the fluctuations due to sources using the techniques of $P(D)$ analysis (Scheuer 1957,1974; Condon 1974; Franceschini et al. 1989; Toffolatti et al. 1998). To begin, we must estimate the cumulative flux distribution of sources, $N(> S) = \int_S^\infty N(S) dS$. The SCUBA results give a list of sources and their fluxes with error bars; they also provide a limit on the low-flux tail of the distribution from their measured residual fluctuations (Hughes et al. 1998). We estimate $N(> S)$ directly, using a Gaussian of width given by the error on the observed flux for each source. We calculate 2σ error bars on $N(> S)$ for this estimated distribution by having the fluctuations in number be consistent with Poissonian fluctuations for each cumulative distribution. We use a top-hat experimental beam to convert $N(> S)$ to an observed flux distribution. We then convert this to the probability distribution, $P(D)$, of getting a total flux, D , in the beam using the elegant formulae of Scheuer (1957; 1974) and Condon (1974). Whereas the integrated background is determined by the slope and low-flux cutoff of $N(> S)$, the anisotropy is dominated by the brightest sources seen by SCUBA.

We consider both the detected sources and the rms noise in the instrument. The observed instrument noise is usually roughly Gaussian with mean near zero. This provides a good upper limit on confusion from undetected sources because one can bury only about half that noise in anisotropy from dim sources without increasing the mean noise level by much or making the noise distribution noticeably non-Gaussian. Hughes et al. report a noise level of 0.45 mJy per 8.5'' beam. To allow for the possibility that a large fraction of this may actually be from sources, we define the total flux, y , the sum of D and this noise contribution. We take the noise distribution to be a zero-mean Gaussian with the reported variance, scaled by the desired beam area. The distribution of y is just the convolution of $P(D)$ and the noise distribution. From $P(D)$ or $P(y)$ we determine the impact on CMB measurements by estimating the variance (σ_D and σ_y). Our 2σ upper and lower limits from SCUBA at 353 GHz are 67 mJy and 8 mJy respectively. Such careful calculations are not strictly necessary; the following easily-reproduced back-of-the envelope calculation is accurate to within a factor of two, adequate for present purposes.

Our upper and lower limits correspond to 2σ confidence levels from the reported observations. If an observational field contains N_{obs} sources, we estimate the upper/lower limit on the number of sources N in a typical such field on the sky using $N_{obs} = N \pm 2\sqrt{N}$, which leads to limits on the fluctuation of the number of sources in a typical field on the sky of $\sqrt{N} = \sqrt{N_{obs} + 1} \pm 1$.

For N sources with flux S per beam, the rms flux anisotropy on the sky is

$$\Delta S = S\sqrt{N} \quad (1)$$

in the Poissonian limit of large N . Toffolatti et al. (1998) predict a negligible contribution from non-Poissonian clustering of sources for beams of $10'$ and larger. Scott & White (1998), however, suggest that clustering will lead to fluctuations twice as large as Poissonian fluctuations for a $10'$ beam, with less enhancement at higher resolution. For $N < 1$ (one source per several beams), we have only a few pixels receiving flux, the mean flux is NS , and

$$\Delta S = \sqrt{N(S - NS)^2 + (1 - N)(NS)^2} = S\sqrt{N - N^2} \quad , \quad (2)$$

which also tends towards $S\sqrt{N}$ as N becomes small.

We extrapolate our upper and lower limits from an observed frequency by using the most extreme known physical emission mechanisms in that frequency range; the fastest the flux should fall is as very steep spectrum synchrotron emission, i.e. ν^{-2} (Steppe et al. 1995), or above 300 GHz as a Wien tail with ν^1 emissivity, i.e. $\nu^3/(\exp(h\nu/kT_{CMB}) - 1)$, since it is unreasonable for a cosmological object to have an effective temperature less than T_{CMB} . Conversely, the fastest a spectrum should be able to rise is as Rayleigh-Jeans thermal emission with ν^2 emissivity, i.e. as ν^4 . Free-free and spinning dust grain emission (Draine & Lazarian 1998) produce less conservative extrapolations.

The way to maximize anisotropy for the observed integrated Far-Infrared Background is to make individual sources as bright as possible. The low emissivity ($\nu^{0.6}$) fit by Fixsen et al. (1998) means that no one graybody spectrum (emissivity between ν^1 and ν^2) can be responsible for the FIRB. Therefore, we set upper limits on the anisotropy at a given frequency by making hypothetical sources whose spectra peak at that frequency be as bright as possible. The brightness of these high- z IR sources is constrained by requiring their dust to have temperature greater than 20K (since low- z inactive spirals have 20K dust) and greater than $3K(1+z)$ (so that the dust is never colder than the CMB at that redshift), and to have a bolometric luminosity no greater than that of a quasar (10^{39} W). We also examine a second model where the luminosity constraint is raised to 10^{41} W, the likely luminosity of APM 08279+5255 once lensing is accounted for (Lewis et al. 1998). Using these constraints, we predict an upper limit of $\Delta T/T = 10^{-6}(10^{-5})$ for a $10'$ beam at 200 GHz for the high- z IR population of luminosity 10^{39} W (10^{41} W) whose total emission generates the FIRB. However, this upper limit is less robust than those from direct observations, because there could be separate source populations, one which yields the integrated background but small fluctuations on the relevant angular scales, and another which dominates the flux anisotropy but produces only a small fraction of the FIRB.

Flux variation, measured in Jy ($1 \text{ Jy} = 10^{-26} \text{ W/m}^2/\text{Hz}$), is converted to antenna temperature T_A by

$$T_A = S \frac{\lambda^2}{2k_B \Omega} , \quad (3)$$

where k_B is Boltzmann's constant, λ is the wavelength, and Ω is the effective beam size.

Small fluctuations in antenna temperature can be converted to effective thermodynamic temperature fluctuations about a mean temperature T_{CMB} using

$$\frac{dT_A}{dT} = \frac{x^2 e^x}{(e^x - 1)^2} , \quad (4)$$

defining $x \equiv h\nu/kT_{CMB}$. This yields an equivalent thermodynamic temperature variation which scales as fwhm^{-1} for a given flux anisotropy on $10'$ scales:

$$\frac{\Delta T}{T_{CMB}} = \Delta S_{10'}(Jy) \left(\frac{\text{fwhm}}{10'} \right)^{-1} (5 \times 10^{-4}) \left(\frac{(e^x - 1)^2}{x^4 e^x} \right) . \quad (5)$$

4. Results

Table 1 shows our upper limits for the possibility of dim sources buried in the instrument noise of non-detections, and Table 2 lists source detections and the resulting limits on $\Delta S_{10'}$. Figure 1 shows our upper and lower limits for flux anisotropy from point sources from 10-1000 GHz, as well as the results for the extreme models of the Far Infrared Background radiation.

We plot the resulting limits on temperature anisotropy in Figure 2 for a range of angular scales and frequencies. The less robust nature of the FIRB constraint prevents us from using this as an upper limit in Figure 2. Because the angular power spectrum C_ℓ of Poissonian distributed point sources increases with multipole ℓ relative to the expected CMB angular power spectrum (Scott & White 1998), an rms $\Delta T/T$ from point sources close to 10^{-5} will seriously impair the measurement of the CMB angular power spectrum on the smallest angular scales, whereas a value less than 10^{-6} means that foreground contamination is not a major concern. The $10'$ lower limit shows that $\Delta T/T < 10^{-6}$ is only possible from 20-300 GHz, and the upper limit for $10'$ shows that $\Delta T/T < 10^{-6}$ at 30 GHz and $\Delta T/T \simeq 10^{-6}$ at 250 GHz. The limits are much less stringent near 100 GHz, where a pathological population of point sources could lead to anisotropy up to 10^{-5} . Typical radio and far-IR sources that fall within these limits at 30 and 250 GHz will end up much closer to the lower limit near 100 GHz, however. Our upper limit constrains all types of point sources, including any hypothetical high-latitude or halo Galactic point sources. Our limits diverge considerably near 100 GHz, so while they are compatible with the model-dependent extrapolations of Blain et al. and Toffolatti et al., they would also be compatible with significantly different extrapolations. Scott & White (1998) indicate that

clustering may lead to a factor of two amplification of our predictions for a 10' beam; the correction is less for higher resolution.

The blank fields observed by VLA, BIMA, IRAM, SCUBA, and CSO were chosen to avoid known bright point sources. Therefore, for observations which avoid known bright sources or mask the pixels containing them, Figure 2 gives full upper and lower limits on point source anisotropy. GS97 and SGMS analyze the contribution of bright IR and radio point sources, respectively, so for a randomly chosen location on the sky the expected anisotropy is the quadrature sum of the anisotropies from those types of bright sources and our result in Figure 2. Figure 3 adds in results for known bright sources from GS97 and SGMS for a 10' beam and shows the results for MAP and Planck after subtracting sources detected at 5σ . Since $\Delta T/T$ is strongly influenced by a few bright pixels due to the highly non-Gaussian distribution, the values are significantly lower after bright source subtraction. Figure 3 shows that for a 10' beam without source subtraction, the point source anisotropy will be $\geq 10^{-6}$ at all frequencies. From 70-200 GHz, the upper limit from Figure 2 dominates the anisotropy from known bright radio and IRAS sources. MAP and Planck can detect the brightest few hundred sources at each frequency (see SGMS) so the upper and lower limits for the satellites diverge over a wider frequency range, making the impact of our uncertainty about the level of anisotropy from dim but numerous point sources a significant problem in predicting foreground contamination. The highest-frequency Planck channels can detect nearly all 5319 IRAS 1.2 Jy sources, so it is the dimmer high-redshift IR galaxies constrained by SCUBA that dominate their source confusion. Our limits here treat each channel independently, but it will be possible to detect bright sources at particular frequencies and mask the corresponding pixels in all channels. This will enhance the importance of dim but numerous sources relative to known bright sources but will reduce the overall level of foreground contamination.

5. Discussion

We find impressive agreement between the SCUBA observations, the IRAM and SCUBA upper limits, and the upper limit for flux anisotropy produced by $10^{39}W$ sources which generate the integrated Far-Infrared Background shown in Figure 1. This is consistent with the FIRB being produced by the SCUBA sources (since the upper limits and the detections differ by only a factor of two), and this indicates that the FIRB sources must be close to maximizing their anisotropy i.e. they are highly luminous but not too numerous. The $10^{41}W$ model, however, predicts more anisotropy than is consistent with the observed SCUBA source counts and IRAM and SCUBA upper limits, suggesting that starburst galaxies like APM 08279+5255 are more luminous than typical FIRB sources. This conclusion is also supported by the near-blackbody spectrum of APM 08279+5255 in the sub-millimeter; there is no way to sum such spectra at various redshifts and produce a graybody of emissivity 0.6 as is seen for the FIRB (Fixsen et al. 1998). The IRAM upper limit is low enough to show that the far-IR sources detected by SCUBA have rising

spectra, so this is further evidence that their emission is thermal in origin.

The CMB anisotropy damping tail on arcminute scales is a sensitive probe of cosmological parameters and has the potential to break degeneracies between models which explain the larger-scale anisotropies (Hu & White, Metcalf & Silk). The expected level of temperature anisotropy is $\Delta T/T \simeq 10^{-6}$, which Figure 2 indicates may be enough to dominate the point source confusion from 30-200 GHz. The upper limit on point source confusion, however, would completely swamp the fluctuations of the damping tail, so more knowledge of dim sources is needed before we can expect such observations to be feasible. A high resolution instrument could use its highest resolution for point source detection and subtraction.

The greatest promise for seeing CMB anisotropies through the obscuration of point source confusion occurs near 100 GHz, but this is also the frequency range where we know the least about the true level of foreground anisotropy on the sky. Our upper limits for $10'$ near 100 GHz give us confidence that useful information will be obtained from CMB anisotropy observations, but it remains possible that point sources will cause thermodynamic fluctuations roughly equal to the intrinsic CMB fluctuations. Since the point source fluctuations come from the highest multipoles, this could seriously impair attempts to measure cosmological parameters from the CMB angular power spectrum. Thus, further high-resolution observations of blank fields at frequencies near 100 GHz are critical in order to determine the actual level of point source confusion, and CMB anisotropy analysis methods must account carefully for contamination from point sources.

6. Acknowledgments

We thank Andrew Blain for his comments on this paper, and Paola Platania, Davide Maino, Gianfranco De Zotti, Carlo Burigana, Malcolm Bremer, and Marco Bersanelli for helpful conversations. E.G. acknowledges the support of an NSF Graduate Fellowship.

REFERENCES

- Aghanim, N., De Luca, A., Bouchet, F.R., Gispert, R., & Puget, J.L. 1997, astro-ph/9705092
- Banday, A.J. et al. 1996, ApJ, 468, L85
- Barger, A.J. et al. 1998, astro-ph/9806317
- Bennett, C.L. et al. 1992, ApJ, 396, L7
- Blain, A.W., Ivison, R.J., & Smail, I. 1998, MNRAS296, L29, astro-ph/9710003
- Blain, A.W., Ivison, R.J., Smail, I., & Kneib, J.-P. 1998, to appear in *Wide-field surveys in cosmology, Proc. XIV IAP meeting*, astro-ph/9806063

- Burigana, C. & Popa, L. 1997, *A&A*, 334, 420
- Carlstrom, J. 1998, private communication
- Church, S. E., Ganga, K. M., Ade, P. A. R., Holzapfel, W. L., Mautskopf, P. D., Wilbanks, T. M. & Lange, A. E. 1998, *ApJ*, 484, 523
- Condon, J.J. 1974, *ApJ*, 188, 279
- Cooray, A. et al. 1998, *AJ*, 115, 1388, astro-ph/9711218
- Draine, B.T. & Lazarian, A. 1998, *ApJL* in press, astro-ph/9710152
- Eales, S. et al. 1998, astro-ph/9808040
- Ferreira, P., & Majaiejo, J. 1997, *Phys. Rev. D*55, 3358
- Finkbeiner, D., Schlegel, D., Davis, M. 1998, in preparation
- Fisher, K.B., Huchra, J.P., Stauss, M.A., Davis, M., Yahil, A., & Schlegel, D. 1995, *ApJS*, 100, 69
- Fixsen, D.J. et al. 1997, *ApJ*, 486, 623
- Fomalont, E.B. et al. 1997, *ApJ*, 475, L5
- Franceschini, A., Toffolatti, L., Danese, L., & De Zotti, G. 1989, *ApJ*, 344, 35
- Gawiser, E. & Smoot, G.F. 1997, *ApJ*, 480, L1 [GS97]
- Grewing, M. 1997, *Proceedings of the ESA Symposium 'The Far Infrared and Submillimetre Universe', 15-17 April 1997, Grenoble, France*, p.219
- Holzapfel, W. 1998, private communication
- Hu, W. & White, M. 1997, *ApJ*, 479, 568
- Hughes, D. et al. 1998, astro-ph/9806297
- Iverson, R. J. et al. 1998, *MNRAS* in press, astro-ph/9712161
- Jaffe, A., & Kamionkowski, M. 1998, astro-ph/9801022
- Kogut, A. et al. 1996, *ApJ*, 464, L5
- Kreysa, E. 1998, private communication
- Lewis, G.F., Chapman, S.C., Ibata, R.A., Irwin, M.J., & Totten, E.J., *ApJL* in press, astro-ph/9807293
- Phillips, T. G. 1997, *Proceedings of the ESA Symposium 'The Far Infrared and Submillimetre Univers', 15-17 April 1997, Grenoble, France*, p. 223
- Puget, J.L. et al. 1996, *A&A*, 308, L5
- Reach, W.T. et al. 1995, *ApJ*, 451, 188
- Refregier, A., Spergel, D.N., & Herbig, T. 1998, astro-ph/9806349
- Richards, E.A. et al. 1998, astro-ph/9803343
- Scheuer, P.A.G. 1957, *Proc. Camb. Phil. Soc.*, 53, 764

- Scheuer, P.A.G. 1974, MNRAS, 166, 329
- Scott, D., & White, M. 1998, astro-ph/9808003
- Smail, I., Ivison, R.J., & Blain, A.W. 1998, ApJ in press, astro-ph/9708135
- Smail, I., Ivison, R.J., Blain, A.W., Kneib, J.-P. 1998, ApJ in press, astro-ph/9806061
- Smoot, G.F. et al. 1992, ApJ, 396, L1
- Sokasian, A., Gawiser, E., Murray, C., & Smoot, G.F. 1998, in preparation [SGMS]
- Steppe, H. et al. 1995, A&AS, 113, 409
- Sunyaev, R.A. & Zel'dovich, Ya.B. 1972, *Comments Ap. Space Sci.* 4, 173
- Tegmark, M. & de Oliveira-Costa, A. 1998, ApJ500, L83, astro-ph/9802123
- Tegmark, M. & Efstathiou, G. 1996, MNRAS, 281, 1297
- Tenorio, L., Lineweaver, C., Hanany, S., & Jaffe, A. 1998, in preparation
- Toffolatti, L. et al. 1995, *Astrophys. Lett.*, 32, 125
- Toffolatti, L. et al. 1998, MNRAS, 297, 117
- Wang, B. 1991, ApJ, 374, 465
- Wilner, D.J., & Wright, M.C.H. 1997, ApJ, 488, L67

Table 1: Noise levels in high-resolution microwave observations. We list the frequency, resolution, noise per beam, and the upper limit for $\Delta S_{10'}$ that results from assuming that half of this noise is really produced by unresolved point sources.

Instrument	ν (GHz)	FWHM	Noise/beam	$\Delta S_{10'}^{upper}$
VLA	8.4	6''	0.0028 mJy	0.14 mJy
BIMA	28.5	90''	0.12 mJy	0.4 mJy
BIMA	107	4.7''	0.7 mJy	45 mJy
SuZIE	142	100''	10 mJy	30 mJy
IRAM	250	11''	0.5 mJy	14 mJy
SCUBA	353	8.5''	0.45 mJy	16 mJy
SCUBA	667	7.5''	7 mJy	280 mJy
CSO	857	10''	100 mJy	3000 mJy

Table 2: Microwave source detections. Upper and lower limits correspond to the observed fields being 2σ Poissonian fluctuations above or below the typical source density on the sky (see text). The totals include the noise totals given in Table 1 added in quadrature with the limits from each source population. The range of sources in the $> 3\text{mJy}$ SCUBA bin allows for the incompleteness correction suggested by Eales et al. and the approximate number in the $1 - 2\text{mJy}$ bin is based on the P(D) analysis of Hughes et al.

Instrument	ν (GHz)	Field size	S_{source}	$N_{sources}$	$\Delta S_{10'}^{upper}$	$\Delta S_{10'}^{lower}$
VLA	8.4	40 sq. '	> 0.5 mJy	3	2.6mJy	0.9 mJy
			0.05-0.5 mJy	8	0.4 mJy	0.2 mJy
			0.009-0.05 mJy	18	0.1 mJy	0.08 mJy
			0.006-0.009 mJy	19	0.04 mJy	0.03 mJy
			TOTAL		2.7 mJy	0.9 mJy
SCUBA	353	46 sq. '	> 3 mJy	15-20	29 mJy	16 mJy
		9 sq. '	2-3 mJy	2	12 mJy	7 mJy
		9 sq. '	1-2 mJy	$\simeq 18$	18 mJy	15 mJy
		TOTAL		40 mJy	23 mJy	

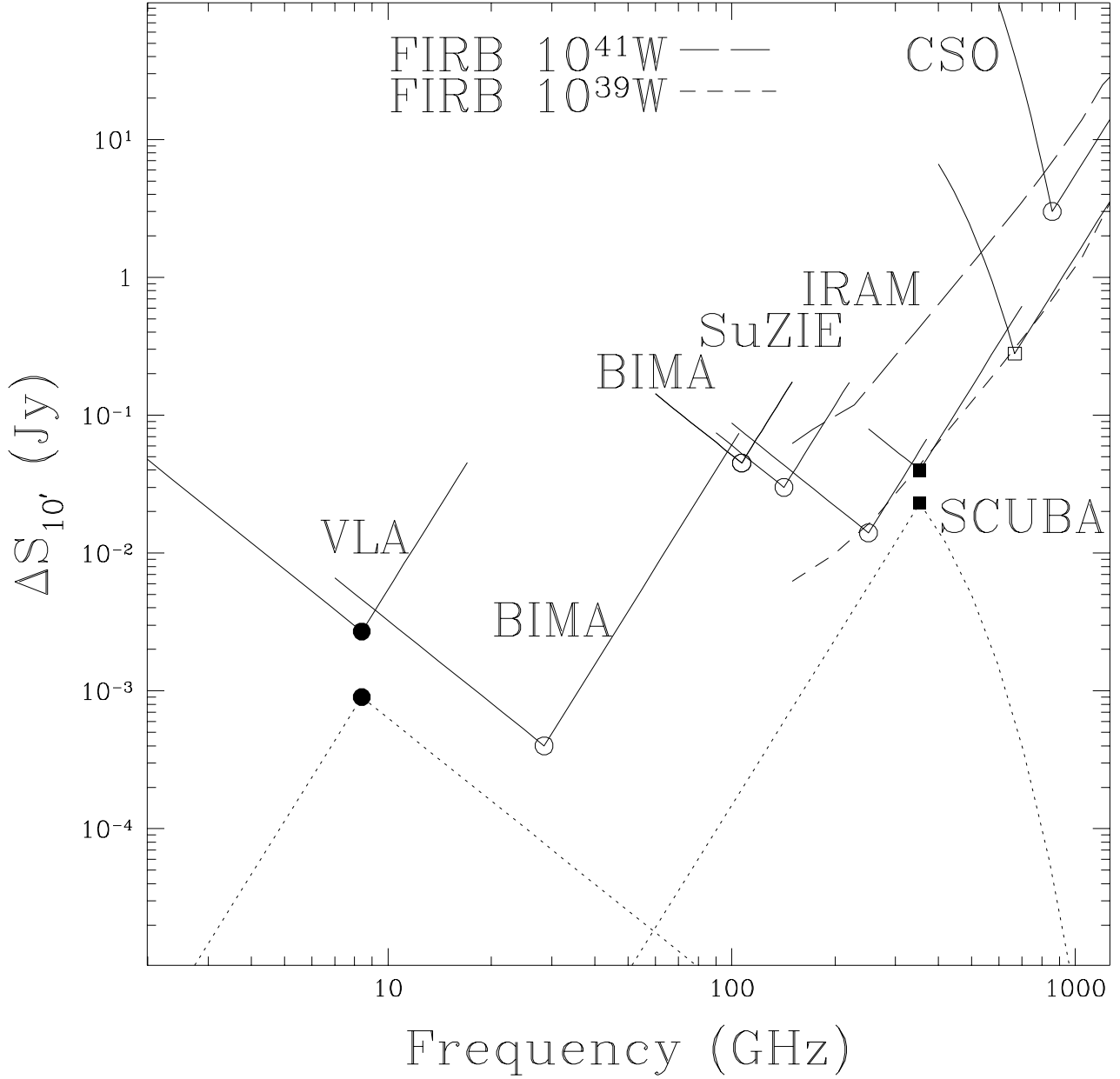


Fig. 1.— Upper (solid) and lower (dotted) limits on flux anisotropy (in Jy) for a $10'$ beam from VLA, BIMA/OVRO, BIMA, SuZIE, IRAM, SCUBA (squares), and CSO. Filled points indicate detections, open points are non-detections, and the extrapolations are based on steep-spectrum radio emission, Rayleigh-Jeans thermal emission with ν^2 emissivity, and Wien tail thermal emission with ν^1 emissivity. The long (short) dashed lines indicate the upper limit on flux anisotropy derived from extreme models of the Far-Infrared Background radiation with a maximum source luminosity of 10^{41} W (10^{39} W).

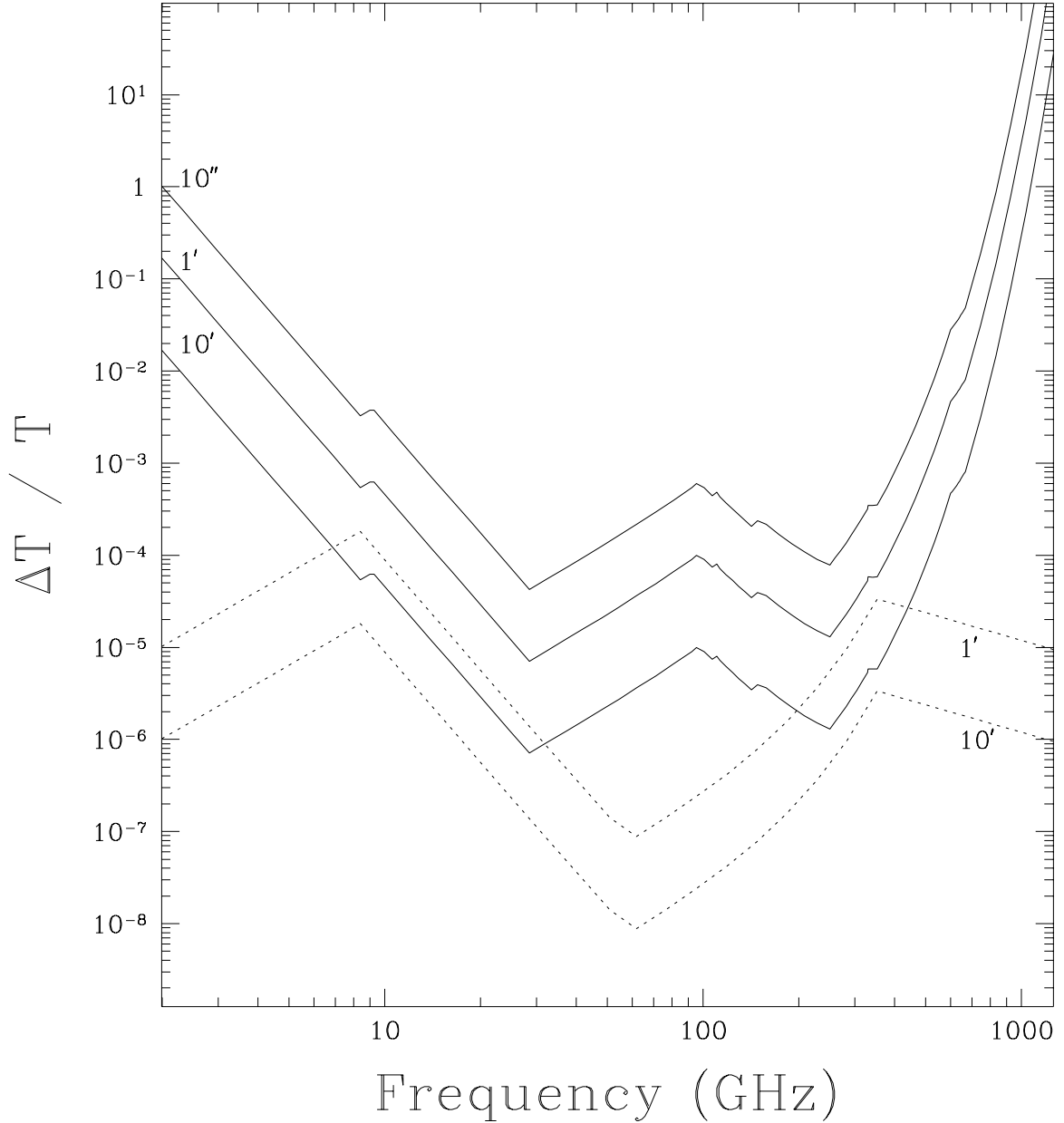


Fig. 2.— Net upper and lower limits on $\Delta T/T$ for $10'$, $1'$, and $10''$ based on the observations and extrapolated limits shown in Figure 1. The lower limit for $10''$ is zero because all sources detected by SCUBA and the VLA should also be detected and subtracted by future observations at that resolution. The upper limits are based on assuming that the combination of instrument noise and CMB fluctuations is too high to subtract any of the SCUBA or VLA sources.

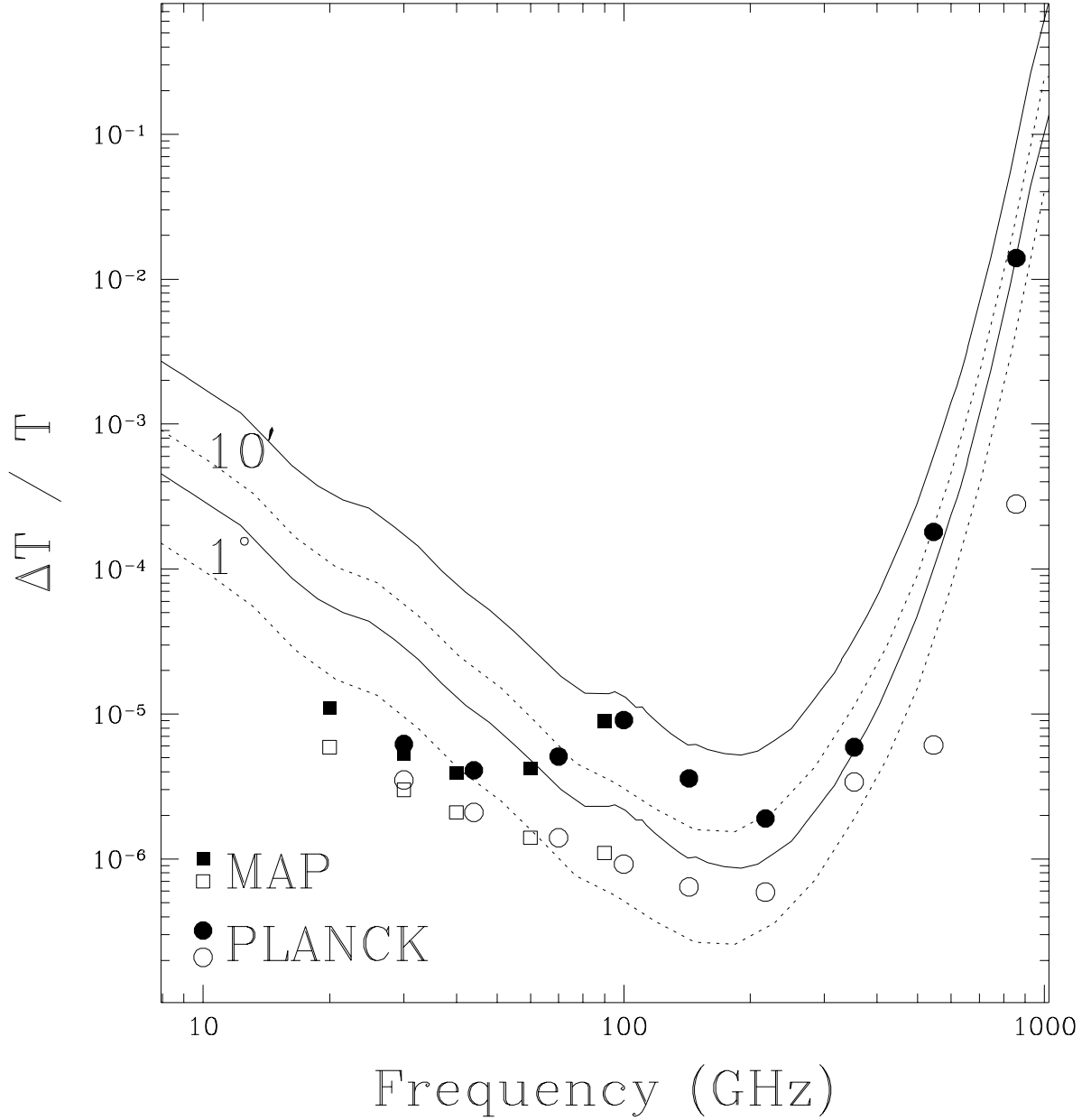


Fig. 3.— Net upper (solid line) and lower (dotted line) limits for $10'$ and 1° , including anisotropy for known bright sources from GS97 and SGMS with a factor of three uncertainty shown. 5σ subtracted upper (solid) and lower (open) limits for MAP (squares) and Planck (circles) are also shown. The channels are treated independently here, although in practice they could be combined to produce somewhat lower anisotropy levels. The combination of pixelization and convolving effects discussed in the text leads to $1/\text{fwhm}$ scaling for all of these point source populations.